JOURNAL OF MATERIALS SCIENCE 35 (2000) 5187–5198

Effect of materials variables on the tear behaviour of a non-crystallising elastomer

K. TSUNODA*, J. J. C. BUSFIELD, C. K. L. DAVIES, A. G. THOMAS
Department of Materials, Queen Mary & Westfield College, University of London, UK
E-mail: c.k.l.davies@qmw.ac.uk

Crack growth rates (r) were measured in pure shear test specimens as a function of strain energy release rate (G) for a non-crystallising SBR elastomer. Measurements were made as a function of: extent of swelling with Dibutyl Adipate; carbon black content; and crosslink density. In some cases experiments were carried out over a range of temperatures. In most cases the resulting G versus r plots showed a clear transition from rough to smooth crack surface behaviour with increasing crack growth rate, with an intervening slip/stick region. In the high speed/steady tear/smooth region the value of G necessary to drive a crack at a given rate was determined largely by the magnitude of the visco-elastic losses in the crack tip region, increasing with: decreasing temperature; increasing molar mass between crosslinks; decreasing extent of swelling; and increasing carbon black content. However G was independent of specimen thickness in this region suggesting that crack tip effects were minimal. In the low speed/rough region changes in the magnitude of G with materials and temperature/rate variables could not be explained by changes in visco-elastic loss alone. Furthermore the magnitude of G increased significantly with increasing specimen thickness. This suggested that in this region cavitation ahead of the growing crack tip resulting from dilatational stresses determined the crack tip diameter, and hence the magnitude of G. © *2000 Kluwer Academic Publishers*

1. Introduction

Crack growth in elastomers has been successfully described utilising a fracture mechanics approach based on the elastic strain energy released as a crack grows. The extensive literature on the subject has recently been reviewed [1, 2]. The strain energy release rate or tearing energy is defined as

$$G = -\frac{1}{t}\left(\frac{\partial U}{\partial c}\right)_l \tag{1}$$

where c is the length of a crack in a body of thickness t and U is the total elastic strain energy stored. G is hence equivalent to the elastic energy released per unit area of one of the fracture surfaces of the crack. G has been found to uniquely describe the tear rate or crack growth rate for a given elastomer for a range of test geometries as described in Fig. 1. The magnitude of G is determined by the visco-elastic work done at the crack tip as a crack propagates [3–7]. This work has been shown [8] to be given by

$$G = W_t d \tag{2}$$

where W_t is the strain energy density at break in the crack tip 'region' and d is equal to the crack tip diameter. It is hence the product of W_t and d which is characteristic of a given crack growth rate for a given elastomer and much work has been carried out in studying the effect of materials and test variables on G, W_t and d. For non-crystallising elastomers the magnitude of G depends strongly on crack growth rate and temperature in a manner which follows the visco-elastic behaviour [3, 5–7, 9] as predicted by the WLF relation [10] with G increasing with increasing rate and decreasing temperature. At the lowest rates and highest temperatures the magnitude of G approaches a threshold value G_0 as the visco-elastic work done asymptotes to zero and the major work to be done is that to break chemical bonds. This situation occurs in highly swollen or very tightly cross linked elastomers particularly at elevated temperatures when the visco-elastic work is at a minimum [11–15]. Under these circumstances the crack tip diameter (d) is also likely to be a minimum, for a very sharp crack, having a value approximating to the distance between crosslinks [11–17]. For most elastomers observed increases in the magnitude of G above G_0 are associated with both visco-elastic effects in W_t and with an increase in the crack tip diameter and associated fracture surface roughness. There is very good evidence, from elegant cutting experiments [18, 19], that crack tip blunting takes place in conventional crack growth experiments at all values of G greater than G_0. Furthermore this tear tip diameter

* On leave of absence from Bridgestone Corporation, Japan.

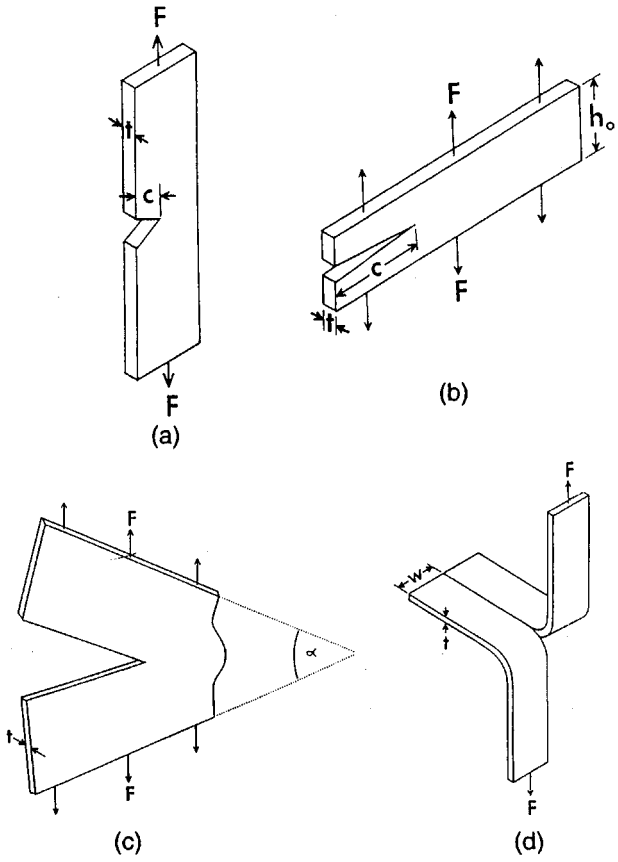

Figure 1 Various crack growth test pieces for which the strain energy density release rate can be measured. (a) tensile – $G = 2kWc$ (b) pure shear – $G = Wh_0$ (c) angled – $G = 2(F/t)\ \sin\alpha/2$ (d) trouser – $G = 2F/t'$.

appears to be function of crack growth rate and temperature in much the same way as the intrinsic visco-elastic properties of the elastomer. The reasons for this roughening effect are not at all clear. In some cases where strength anisotropy may be introduced at the crack tip due to pre-strain or orientation of particle filler networks the roughening may be due to subsequent crack deviation [9, 21]. In non-crystallising elastomers changes in the tear behaviour are often associated with distinct changes in surface roughness as illustrated in Fig. 2. At high rates of tear (region C) surfaces are very smooth, like a glassy fracture, and cracks grow at a constant rate

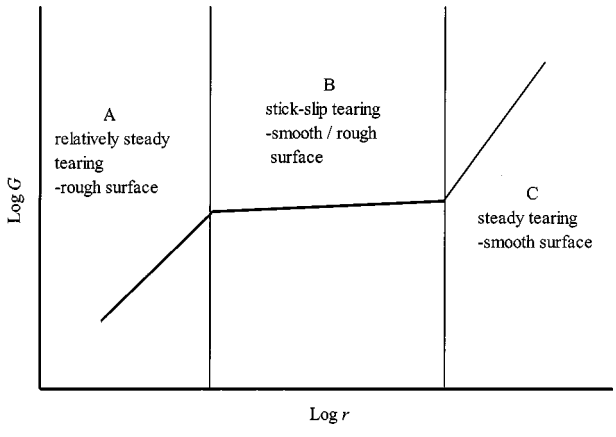

Figure 2 Schematic Figure illustrating the strain energy release rate (G) tear rate (r) relationship for a non-crystallising elastomer.

in a manner controlled by the visco-elastic behaviour of the elastomer, being scaled by the WLF relationship [5, 9, 22]. At low rates of tear (region A) the tearing is fairly steady but the crack surface is now clearly rough. In region B tearing takes place in a stick/slip manner with a resultant rough/smooth surface. This abrupt change in tear behaviour from region C to A is clearly associated with surface roughening due to crack tip blunting. It has been shown that under hydrostatic tension elastomers can cavitate at a stress of the order of the tensile modulus [23–29]. Such stresses can exist ahead of a growing crack tip and it has been suggested [22, 30–32] that the surface roughness observed in region A results from the intersection of the propagating crack with growing cavities. At high tearing rates in region C it is suggested that the elastic modulus ahead of the crack tip is increased substantially suppressing cavity growth. Evidence to support this hypothesis has been provided by crack growth rate experiments carried out in samples subject to hydrostatic pressures [30–32]. In these the transition from rough to smooth crack growth behaviour occurs more easily as the pressure increases and cavitation is 'suppressed'.

The present work was undertaken in an attempt to further our understanding of the transition in tearing behaviour illustrated in Fig. 2, particularly in light of concepts of cavitation behaviour. It was proposed to carry out tearing experiments on a non-crystallising elastomer, SBR, with widely different visco-elastic properties, to be achieved by swelling with liquids, varying the temperature and crosslink density and filling with carbon black. The tests with swollen materials were an extension of work by the authors on the effect of swelling on visco-elastic loss in strained elastomers [33, 34]. Hence, the main purpose of the current experiments was to study the effect of the magnitude of visco-elastic loss on the rough to smooth transition and hence crack tip behaviour. Finally, crack growth rate experiments were to be carried out on specimens of varying thickness which would have continuously reducing dilatational stresses ahead of a crack tip as the specimen thickness decreased and hence, a reduced propensity to cavitate.

2. Experimental

All tests were carried out using a styrene-butadiene copolymer (23.5% Styrene, SBR 1502, JSR). Sheets were hot pressed and cross linked to various degrees using either dicumyl peroxide or a sulphur vulcanising system at 160°C for 30 minutes as indicated in Table I. In most cases sheet thicknesses of 1mm were prepared but sheets of various thicknesses from 2.0 mm to 0.1 mm were manufactured to study the effect of thickness on crack growth behaviour. Some sheets were manufactured containing 10 or 50 parts by mass of carbon black (N330- HAF) to 100 parts by mass of the elastomer, SBR. Following cross linking some compounds were swollen to contain various volume fractions of elastomer with Dibutyl Adipate. All formulations and some physical properties of the compounds are given in Table I. The average molar mass between crosslinks (M_c) was determined using tensile

TABLE I Compound formulations Styrene Butadiene Rubber

		SBR-A	SBR-B	SBR-C	SBR-D	SBR-E	SBR-F	SBR-G	SBR-H	SBR-I	SBR-J
Styrene Butadiene Rubber	SBR #1502	100.0	100.0	100.0	100.0	100.0	100.0	100.0	100.0	100.0	100.0
Carbon Black (HAF)	N330					10.0	50.0				
Stearic Acid		2.0	2.0	2.0	2.0	2.0	2.0				
Zinc Oxide		5.0	5.0	5.0	5.0	5.0	5.0				
Antioxidant/antiozonant	6PPD	3.0	3.0	3.0	3.0	3.0	3.0				
Sulphur		0.5	1.0	1.5	10.0	1.5	1.5				
Dicumyl Peroxide								0.1	0.3	0.5	5.0
Accelerator	DPG	1.3	1.3	1.3	1.3	1.3	1.3				
Accelerator	MBTS	1.0	1.0	1.0	1.0	1.0	1.0				
Sp. Gr.	g/cm^3	0.987	0.989	0.991	1.030	1.065	1.181	0.940	0.940	0.940	0.940
Curing Condition		160°C × 30 min									
$M_{c\,pysc.}$	g/mol	66428	22266	9889	1084			77890	13592	5917	862

stress-strain measurements and the relationship between the Mooney-Rivlin constant C_1 and M_c.

The majority of crack growth rate measurements were carried out using a 'pure shear' test piece (Fig. 1b) with a small number being carried out with a trouser test piece (Fig. 1d). Both test pieces were usually 1 mm in thickness.

Pure shear test pieces were 20 mm in height and 200 mm long. Crack growth rate measurements were only conducted on cracks of sufficient length to be growing in the pure shear region of the test piece as determined by finite elements analysis (FEA). The strain energy release rate or tearing energy was calculated for each crack growth rate (each specimen extension) using the relationship

$$G = Wh_0 \tag{3}$$

where W is the strain energy density in the central region and h_0 is the unstrained height. W is given by the total elastic energy stored divided by the volume of the uncracked part of the specimen. A slight adjustment to this volume needs to be made to allow for the load carrying capacity around the crack tip. This was carried out by calibration as reported previously [35]. The magnitude of the elastic energy stored for each specimen extension was calculated by determining the stress-strain curve for the specimen and integrating the function which represented the curve to the appropriate specimen extension.

The trouser test pieces were 30 mm wide and 60 mm in length. They were precracked to a length of 30 mm. They were extended at various rates and the resultant tear force (F) measured. The strain energy release rate was calculated using the relationship

$$G = \frac{2F}{t'} \tag{4}$$

where t' is the tear path determined by the angle of crack growth given approximately by $t\sqrt{2}$ where t is the specimen thickness. It was assumed that the extension of the legs of the trouser test piece was negligible.

The mechanical measurements were carried out on either a static simple loading frame or an Instron screw driven testing machine. A few cyclic crack growth rate experiments were carried out at a frequency of 5 Hz using a servo hydraulic machine. Crack lengths at a given time and hence crack growth rates were determined using a scale printed on the specimens and a video camera/recorder.

The dynamic mechanical properties, particularly E'', were measured using a simple oscillating beam apparatus described previously [33, 36]. The apparatus provides accurate measurements of E'' for low visco-elastic loss materials, particularly swollen elastomers.

All fracture surfaces were examined with the naked eye and with an optical microscope. Optical micrographs were taken of the fracture surface and normal to main face of the pure shear test specimen, containing the line of the crack.

3. Results and discussion

The effect of materials variables on the tearing behaviour will be reported under four headings which represent the major variables studied. Unless otherwise stated the results correspond to pure shear test data particularly from the compound SBR-C. The tear rate/strain energy release rate data will be described in terms of Fig. 2 utilising regions A,B,C.

3.1. Swelling liquid effects

The work reported here is a small part of a larger study carried out by one of the authors, K. Tsunoda, on the effect of the viscosity of a swelling liquid on the tearing behaviour of elastomers. It is included here to illustrate the effect of swelling on the visco-elastic behaviour and the static and cyclic crack growth behaviour. For this purpose only the results for a relatively low molar mass, low viscosity liquid, Dibutyl Adipate (DBA) are reported.

Fig. 3 shows a plot of the Dynamic loss modulus (E'') for various extension ratios for the SBR-C swollen with DBA. The magnitude of E'' is seen to decrease by a factor of 10 for the swollen material, which contains only a 0.4 volume fraction of elastomer. This measure value, while very low is still larger than that measured by the authors for natural or synthetic *cis*-polyisoprene under similar circumstances. Fig. 4 shows the strain energy release rate (G) for these materials at three tearing rates determined using trouser test pieces. The energy necessary to drive a crack is seen to fall continuously with

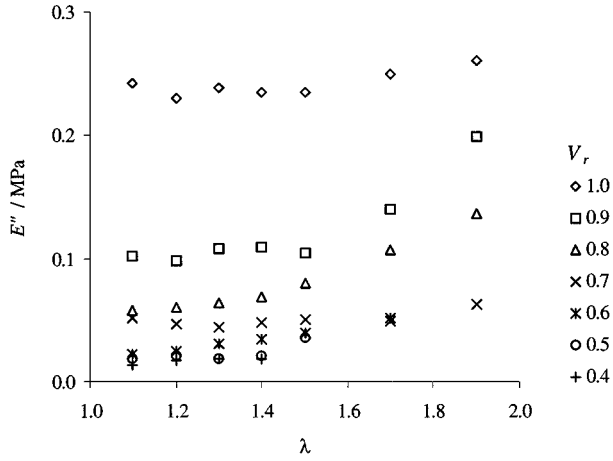

Figure 3 The dynamic loss modulus (E'') for SBR-C swollen with Dibutyl Adipate as a function of extension ratio (λ).

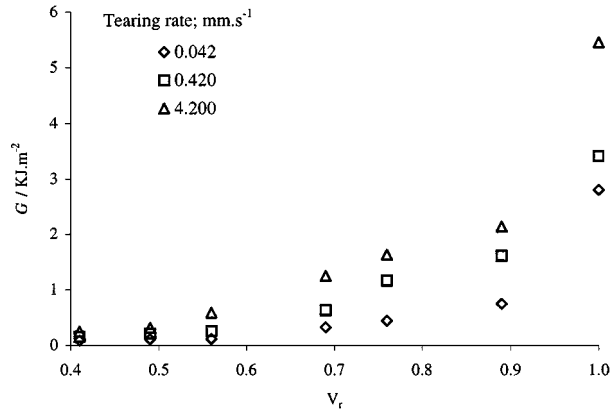

Figure 4 The strain energy release rate (G) for SBR-C swollen with Dibutyl Adipate as a function of volume fraction of elastomer (V_r) at various tear rates in a trouser test piece.

increasing swelling i.e. decrease in volume fraction of elastomer. The results for the 0.42 mm/s tests are shown plotted against the appropriate loss modulus in Fig. 5. At this rate mostly smooth tear surfaces are produced. As expected the necessary energy release rate increases continuously as the swollen elastomer becomes more visco-elastic. Under these circumstances this is more likely to result from an increase in W_t (Equation 2) due to the increase in energy losses rather than to continuous changes in crack tip geometry. The rate dependence of G which still remains even for the most highly swollen material in Fig. 4 suggests that at 20°C visco-elastic losses still raise the measured value of G above the threshold value G_0. To investigate this tear tests were carried out for the most highly swollen material at temperatures of 20°–80°C at various rates as illustrated in Fig. 6. It can be seen that at 40°–80°C the measured value of G becomes essentially independent of tear rate and hence yields a value of G_0 of 60 J·m^{-2}. This is in line with previously determined experimental values for a range of materials [11–15] and theoretical predictions [11–17] and hence gives confidence in the sensitivity of the current measurements. The tear data for the material highly swollen with DBA determined with pure shear test pieces at 20°C is given in Fig. 7. At imposed values of G below 50 J m^{-2} no tearing was observed during the time scale of the experiment. This value of G is consistent with the value of G_0 determined from the trouser test results. Finally crack growth rates for the material swollen with DBA

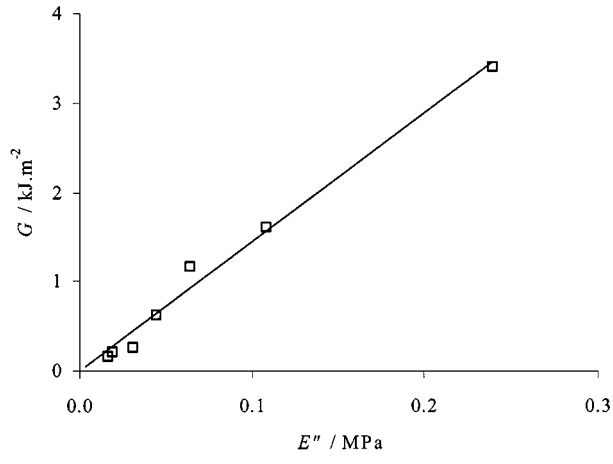

Figure 5 The strain energy release rate (G) for SBR-C swollen with Dibutyl Adipate for a trouser test piece at a rate of tear of 0.42 mm·s^{-1} as a function of the measured dynamic loss modulus (E'').

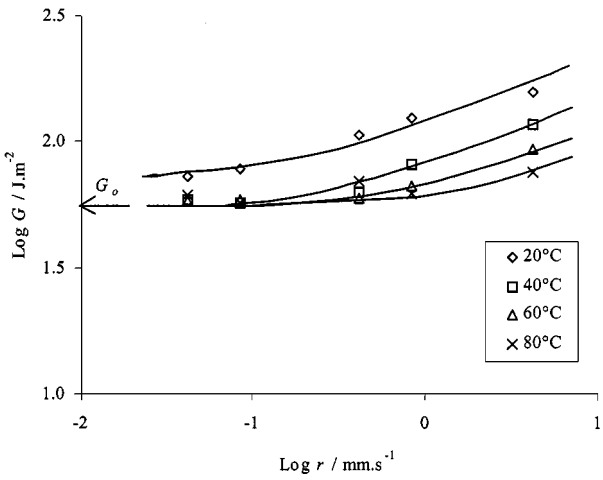

Figure 6 The effect of temperature and extension rate on the strain energy release rate (G), tear rate (r) relationship for trouser test pieces of SBR-C swollen with Dibutyl Adipate to (V_r) = 0.38.

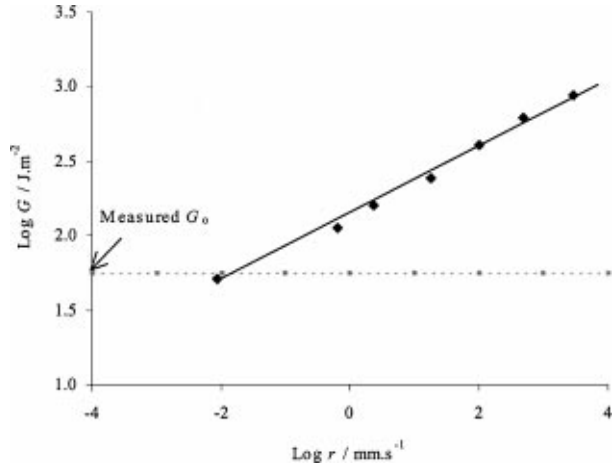

Figure 7 The tear rate (r) as a function of the strain energy release rate (G) for SBR-C as in Fig. 6 for pure shear test pieces showing the threshold for crack growth G_0.

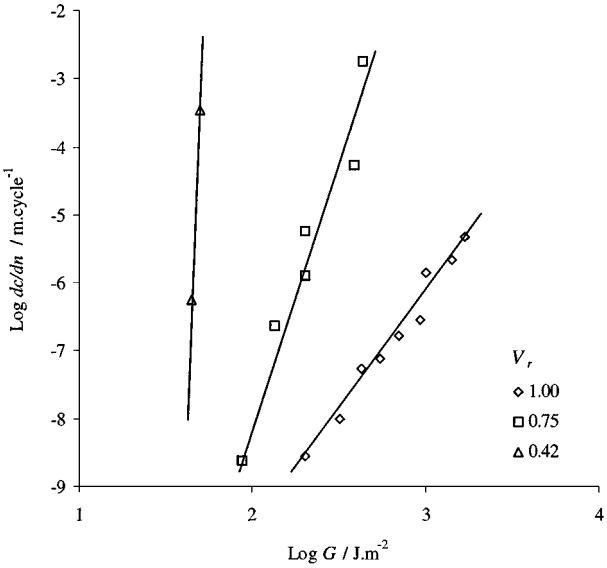

Figure 8 The effect of swelling SBR-C with Dibutyl Adipate on the cyclic crack growth rate (dc/dn) strain energy release rate (G) relationship.

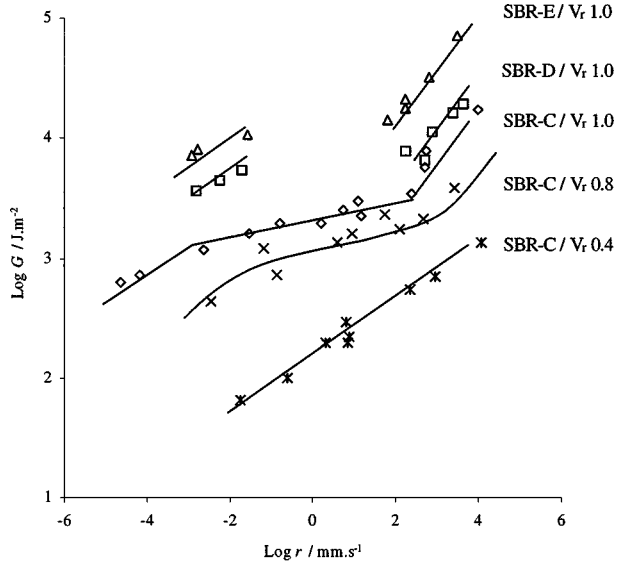

Figure 9 The tear rate (r) as a function of the strain energy release rate (G) for a series of HAF carbon black filled or Dibutyl Adipate swollen SBR-C compounds.

were measured in pure shear test pieces tested cyclically at 5 Hz, the results of which are given in Fig. 8. The amount of crack growth per cycle (dc/dn) is seen to increase dramatically for a given strain energy release rate as the extent of swelling increases and the visco-elastic loss decreases. Crack growth in the most highly swollen material does not quite become catastrophic as the magnitude of the necessary energy release rates at 20°C remains larger than G_0, as shown in Fig. 7.

All the data reported in this section are consistent with time dependent crack growth in SBR being controlled by visco-elastic loss in the crack tip region, with the role of the swelling liquid being to markedly reduce this loss process. The measured G_0 value is consistent with previously published data [11–15] as is the cyclic and static crack growth behaviour in the region of G_0. The role of the swelling liquid will be discussed further in the next section when the effects of other materials variables are included.

3.2. Effect of carbon black addition and swelling on the behaviour at various temperatures

The tear rate (r) as a function of the strain energy release rate for the SBR compounds cross linked with 1.5 parts of sulphur and containing various parts of either carbon black or swelling liquid is shown in Fig. 9. In general the effect of addition of carbon black is to increase the tearing energy necessary to drive a crack and that of the swelling liquid is to cause a reduction. As discussed in the introduction these changes could result from energy loss effects in W_t or from changes in the crack tip diameter d and associated crack surface roughness or from a combination of both effects. In an attempt to gauge changes in crack tip behaviour optical micro-graphs were taken of fracture surfaces as illustrated in Fig. 10. Micro-graphs were taken from regions A, B, C or boundaries between the regions as indicated on Fig. 10.

The unfilled /non-swollen SBR-C shows a very clear change from smooth behaviour at high tear rates in region C to rough behaviour at low rates of tear in region A. In the intervening region B, a mixed behaviour is seen. In this region stick/slip crack propagation occurs with the crack growing in slow and fast bursts. It is the average values of these combined crack growth rates which are plotted on Fig. 9, averaged over a crack growth length of $C_{\text{Total}} = 160$ mm. In each region actual crack growth rates were measured over much shorter crack growth increments (C_I) and these results are shown plotted in Fig. 11 in the form of histograms of crack growth frequency (C_I/C_{Total}) against incremental crack growth rate. In region C the distribution is narrow and cracks are seen to grow at a very precise rate. In region A the distribution is broader but the crack growth rate can reasonably be represented by a mean or average value. In region B the distribution is clearly bimodal and cracks either grow at a slow or fast rate. These fast and slow rates are plotted together with the average rate in Fig. 12. It is clear that cracks grow in this transition region at rates associated with either the high energy/high rate process or the low energy/low rate process as was originally reported [22]. It was as a result of this phenomenon that the original suggestion was made that the low rate process involved significant cavity growth ahead of the crack tip, which was suppressed at high rates [22, 30–32], hence causing significant changes in effective crack tip diameter. The present work was intended to extend this previous study and the procedure described above was an important vehicle in this respect. Hence a large number of measurements of this type were made, only some of which will be illustrated here.

Measurements were made of the temperature dependence of the strain energy release rate versus tear rate relationship for this unfilled/non swollen SBR material as illustrated in Fig. 13a. As expected the strain energy release rate necessary to drive a crack at a given rate decreases with increasing temperature as the visco-elastic

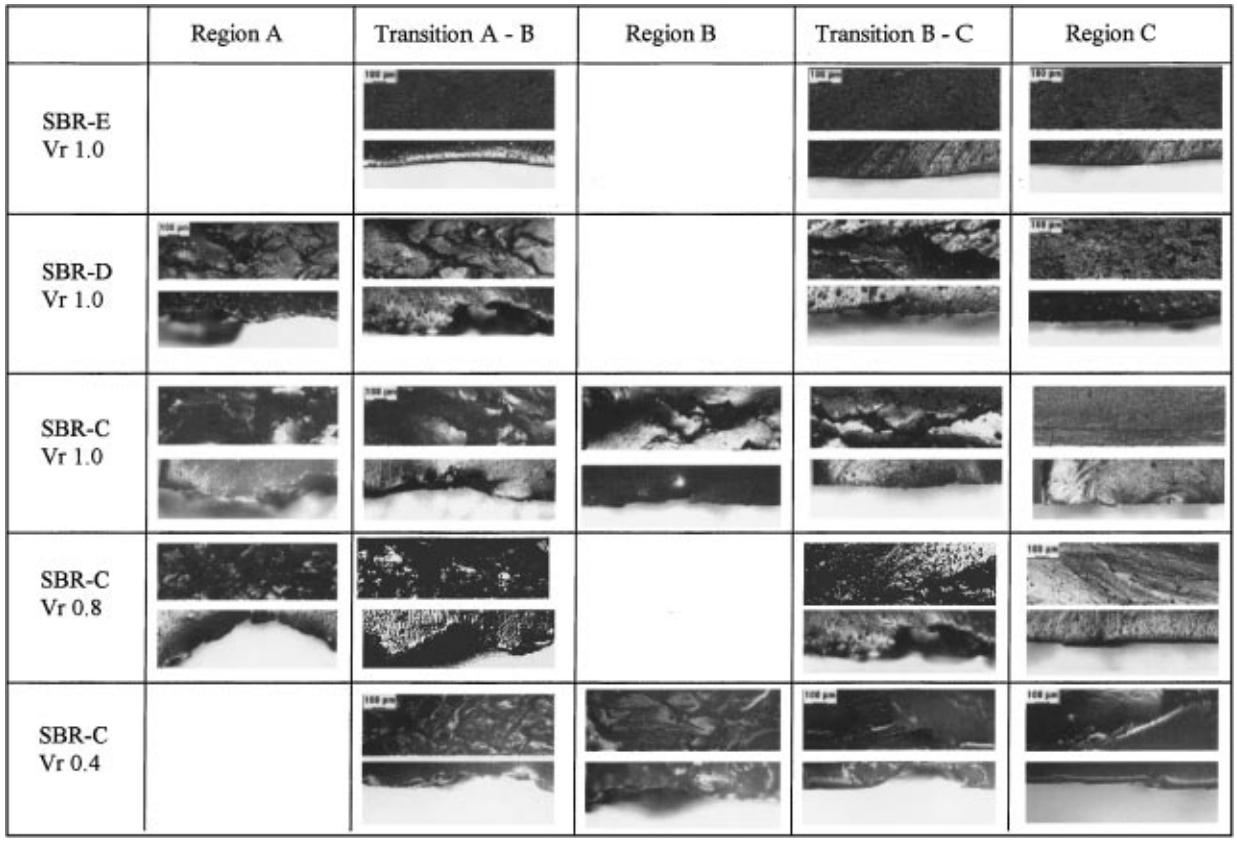

Figure 10 Optical micrographs of the fracture surfaces of the specimens used to generate Fig. 9. The crack propagation direction is right to left.

work necessary decreases. These data are shifted using the usual form of the WLF relationship

$$\log a_T = \frac{-8.86(T - T_s)}{101.6 + T - T_s} \tag{5}$$

with $T_s = T_g + 50^\circ$C as indicated in Fig. 13b. The data clearly tend to superpose particularly in the smooth and slip/stick tear regions. The fact that they superpose in the steady/smooth tear region is not surprising as the large visco-elastic losses at these tear rates are likely to dominate the crack growth process [3–7]. The superposition in the stick/slip region is more surprising as it would be expected that variation in crack tip behaviour would play a role. However, it has been suggested that even the variation of crack tip diameter scales with changes in the visco-elastic behaviour [19].

The addition of carbon black to this SBR compound clearly causes an increase in strength (Fig. 9). It also introduces a discontinuity into the strain energy release rate data as average crack growth rates over a region of nearly four orders of magnitude do not occur. Cracks either grow slow or fast with no slip/stick region within which to generate average values. For both filled materials the fracture surfaces at high rates of tear are smooth (Fig. 10). At lower rates of tear the surface of the 10 phr carbon black filled SBR is rough and it behaves more like the unfilled material. However the surface of the 50 phr carbon black filled material is always relatively smooth, and if cavitation occurs the cavities must only open up to a small extent. Crack growth rate experiments were carried out at various temperatures using the 10 phr carbon black material, the results of which are given in Fig. 14a. The effect of increasing the temperature is clearly to reduce the strain energy release rate necessary to drive a crack. In addition, the discontinuity in crack growth rates is not observed at elevated temperatures. An attempt was made to superpose these data as illustrated in Fig. 14b. The superposition works at high crack growth rates where smooth surfaces are produced. In this region it is possible that the tear tip diameter changes little with temperature and rate and that the temperature dependence of crack growth rate arises purely from the decrease in the visco-elastic work that is done, as the temperature increases. At low crack growth rates, in the slip/stick or rough regions no superposition occurs. This suggests that in these regions the variation of the crack tip diameter is important. It is possible that at high crack growth rates the role of carbon black is to markedly increase the hysteretic losses, resulting in significant increases in W_t [37]. However at low crack growth rates it may be major changes in the crack tip profile which are important [38]. What is not clear is why a discontinuity in crack growth rate is observed for these materials at 20°C but is not observed at elevated temperatures. If cavitation ahead of the crack tip is important at low crack growth rates, it may be that in filled materials cavities are more numerous opening up at inherent flaws or filler particle aggregates. At the same time cracks need a large energy to drive them due to the larger hysteretic losses in the crack tip region. The result would be that the crack tip would intersect many growing cavities causing considerable blunting. A small increase in strain energy release rate in this region would be enough to increase the rate of crack growth so that voids grew very little before being

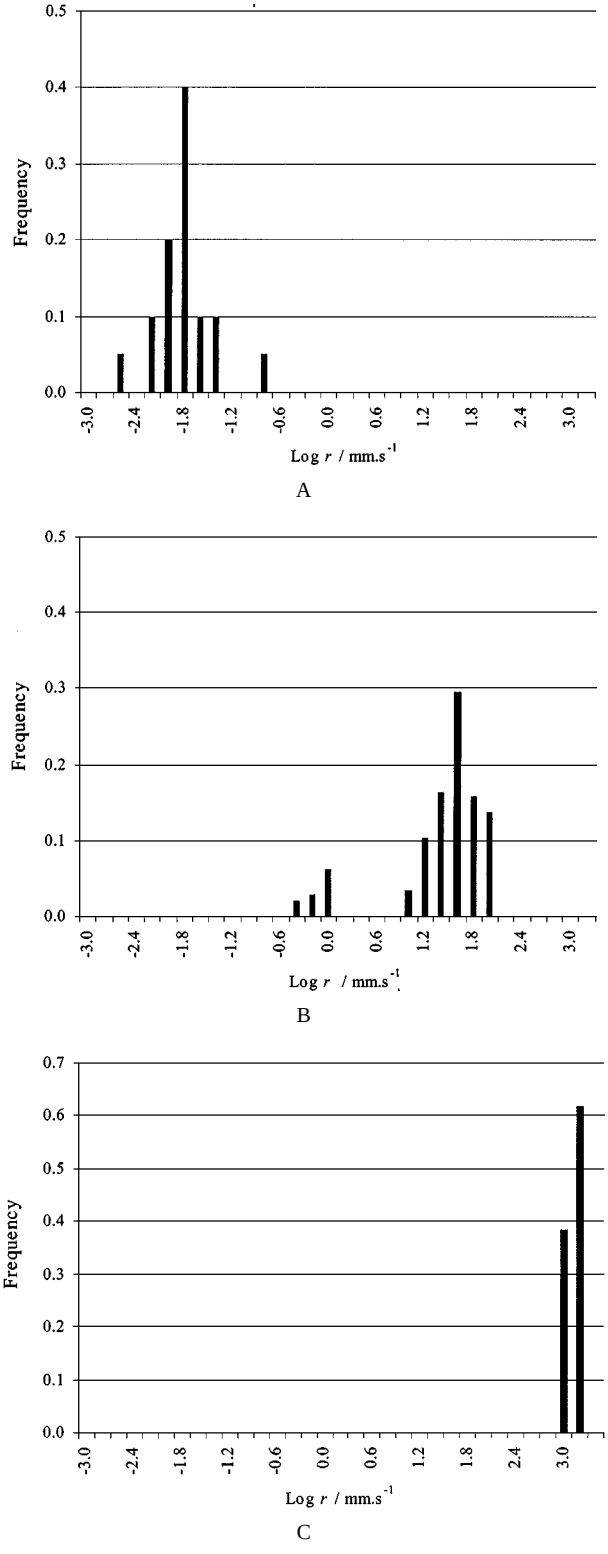

Figure 11 Frequency distribution of tearing rates for SBR-C in regions A, B, C. A-Rough/Steady. B-Stick/Slip. C-Smooth/Steady.

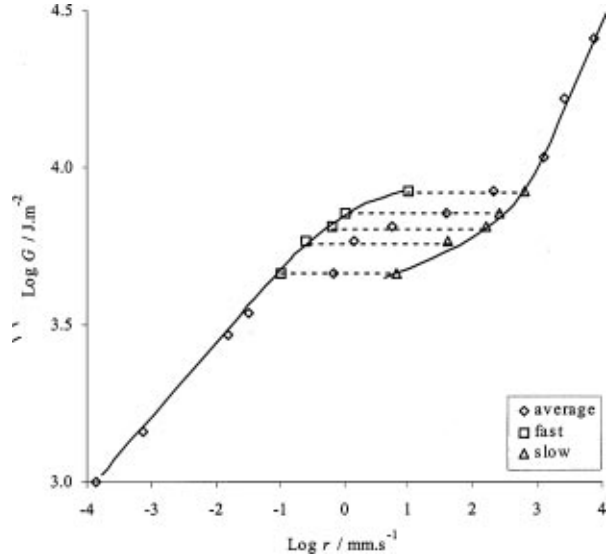

Figure 12 The tear rate (r) a function of strain energy release rate (G) for SBR-C showing the average, fast and slow rates in the stick/slip region.

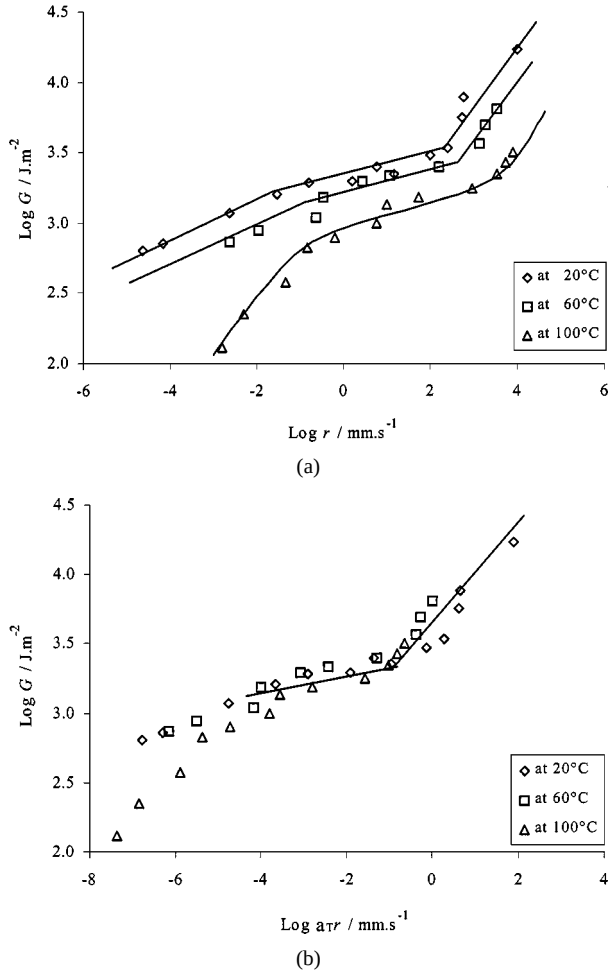

Figure 13 (a) The effect of temperature on the strain energy release rate (G) versus tear rate (r) relationship for unfilled SBR-C. (b) Attempted superposition of the data given in Fig. 13a using the WLF shift factor (a_T) as given in the text.

absorbed by the advancing crack tip. This would then cause the dramatic increase in crack growth rate of four orders of magnitude. It appears that increasing the temperature reduces the hysteretic losses enough to allow a slip/stick situation to reappear where cavities do or do not intersect with a crack in a semi random manner over the transition region.

The crack growth behaviour in the swollen materials is by no means simple. Clearly swelling reduces the observed crack growth rates for a given energy release rate as would be expected from the reduction in visco-elastic losses. However while the behaviour of the material swollen to a $V_r = 0.8$ follows the general pattern of slip/stick behaviour (Fig. 9) and of a rough to smooth transition with increasing rate (Fig. 10), the

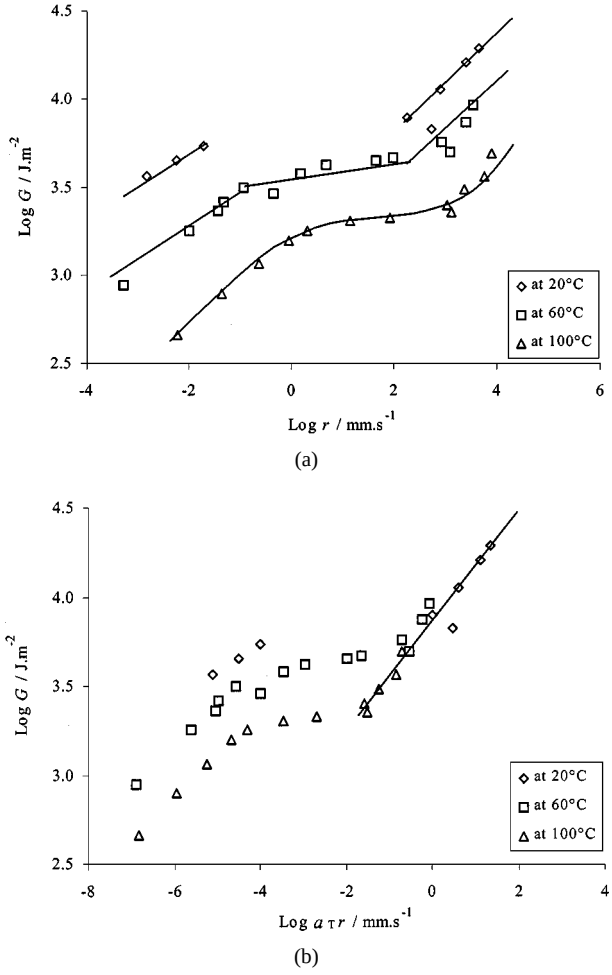

Figure 14 (a) The effect of temperature on the strain energy release rate (G) versus tear rate (r) relationship for SBR-C filled with 10 phr HAF carbon black (compound D). (b) Attempted superposition of the data given in Fig. 14a using the WLF shift factor (a_T) as given in the text.

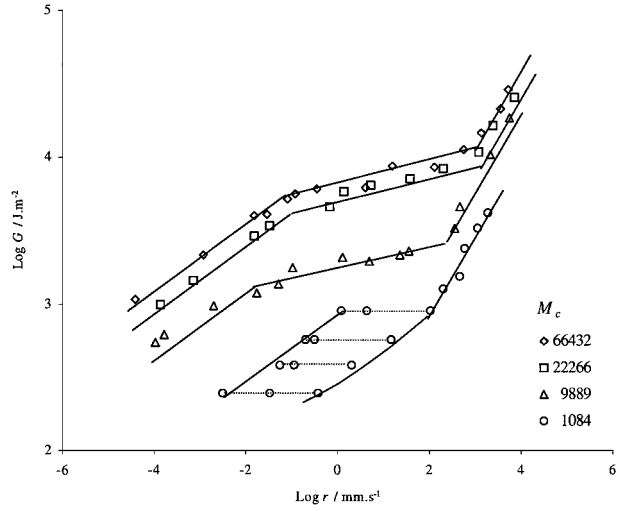

Figure 15 The effect of the average molar mass between cross-links on the strain energy release rate (G) versus tear rate (r) relationship for SBR cross-linked with sulphur.

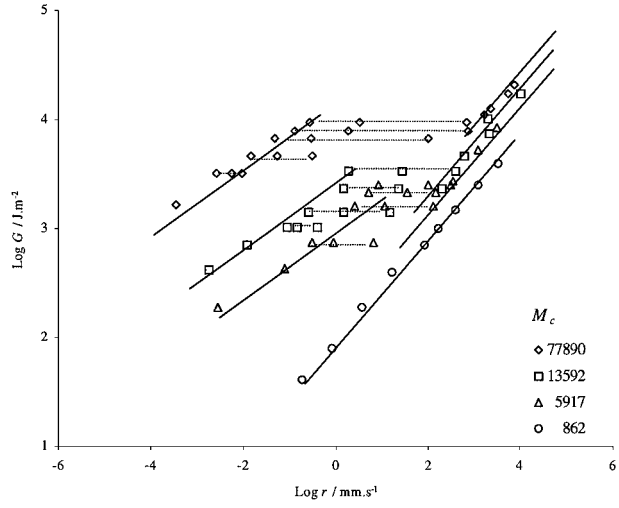

Figure 16 The effect of the average molar mass between cross-links on the strain energy release rate (G) versus tear rate (r) relationship for SBR cross-linked with dicumyl peroxide.

highly swollen material appears to show mostly rough surfaces but maybe with some rough/smooth transition (Fig. 10) but with no slip/stick region (Fig. 9). It is possible that in very low loss materials with cracks growing at relatively low strain energy release rates that cavitation ahead of the crack tip occurs to some extent most of the time.

It is clearly qualitatively possible to explain some of the effects observed in terms of cavity formation ahead of a crack tip for the filled and unfilled SBR materials. It is also likely that hysteretic losses are the main contributor to G via W_t at high crack growth rates and crack tip blunting is the main contributor to G via d at low crack growth rates. However quantifying the relative contributions is clearly very difficult.

3.3. Role of molar mass between crosslinks

The relationship between the strain energy release rate and the crack growth rate for materials of varying crosslink density is shown in Fig. 15 for SBR crosslinked with sulphur and in Fig. 16 for SBR crosslinked with dicumyl peroxide. The materials exhibit a slip/stick transition region. However the extent of this region decreases with decreasing molar mass between crosslinks for the peroxide cured materials, with the region not being observed in the material of lowest molar mass between crosslinks. At high rates of tear all the materials exhibit very smooth surfaces with rough surfaces being observed at low rates, with a mixed transition region. In addition in the rough region the extent of roughness increases with increasing molar mass between crosslinks. In all cases the slow, fast and average crack growths rates were determined for each value of G in the transition region. All three values are only plotted on the graphs where space allows. It is clear, however, that the transition region consists of increments of crack growth by either the fast or slow crack growth process.

The strain energy release rate necessary to drive a crack at a rate of 1 m/s in the smooth growth region is plotted as a fraction of the molar mass between crosslinks in Fig. 17, for both the peroxide and sulphur cured materials. A line of slope 1/2 is drawn on the figure corresponding to

$$G \propto M_c^{1/2} \qquad (6)$$

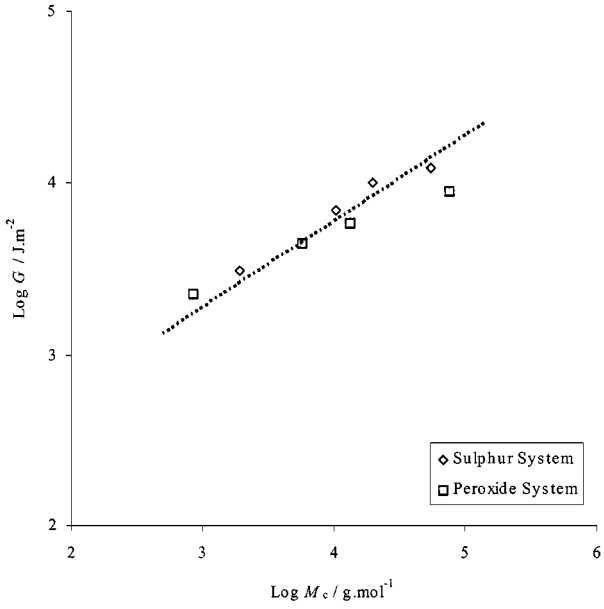

Figure 17 The variation of the strain energy release rate (G) with the average molar mass between cross-links for sulphur and peroxide cured SBR during smooth steady tearing at 1.0 m/s.

A similar relationship was found by Gent *et al.* [19] for an SBR material where G was measured via a cutting experiment, with essentially a crack tip diameter independent of crack growth rate. However the strain energy release rate necessary to drive a crack at a given rate has been found to be greater in systems with poly-sulphidic crosslinks than in systems with short C–C crosslinks resulting from peroxide curing [18, 9, 39]. However in the present case, in the smooth growth region, the strain energy release rate depends to a first approximation only on the molar mass between crosslinks. The degree of crosslinking has been shown theoretically to increase the threshold strain energy release rate as

$$G_0 \propto M_c^{0.5} \tag{7}$$

At the high rates of tear observed in the smooth growth region it would appear that cracks grow with a relatively fixed crack tip geometry at a rate determined by the visco-elastic losses, which scale with the threshold strain energy release rate G_0. The contribution of the polysulphidic crosslink chains to this energy loss in this region must be small although perhaps not negligible if the relative slopes for the peroxide and sulphur cured materials in Fig. 17 are compared.

In the rough region changes in the crack tip diameter must make some significant contribution to the strain energy release rate. It has been suggested that changes in the tip diameter will scale with changes in the visco-elastic losses [19], increasing as the visco-elastic loss increases. This may be true in the present case with the resulting strain energy release rate necessary to drive a crack increasing rapidly with increasing molar mass between crosslinks (Figs 15 and 16). If the change in crack tip diameter is associated with cavitation ahead of the crack tip it may be that in the more visco-elastic materials (higher molar mass between crosslinks) the slower crack growth rate allows cavities to grow to a greater size before they are intersected by the crack tip.

The reason for the decrease in the extent of the slip/stick transition zone with increasing crosslink density is not clear. The effect is greatest for the peroxide cured materials with no transition being observed in the G versus r plot for the highest crosslink density material. This is the least visco-elastic material and a similar behaviour is observed for the most highly swollen material (Fig. 9) with both showing some rough/smooth transition. It is tempting to suggest that as the materials become less visco-elastic the crack growth rate for a given strain energy release rate increases and the effect of cavity growth ahead of the crack tip continuously decreases, this process continuing until in very low loss materials any cavity growth which occurs has a minimal effect, resulting in the elimination of the transition region. This effect would occur earlier for the peroxide cured materials, as the C–C crosslinks would contribute little to the visco-elastic losses compared to the polysulphidic crosslinks [18, 19, 39].

3.4. Specimen thickness effects

The effect of specimen thickness on the strain energy release rate versus crack growth rate relationship for sulphur cured SBR-C is shown in Fig. 18a. Only average values of crack growth rate are plotted on this figure in the slip/stick region due to shortage of space. However, the slow/fast/average values are plotted for the thinnest specimen in Fig. 18b. It is clear that the specimen thickness has no effect on the measured crack growth rates during steady/smooth tearing. However, a continuous decrease in crack growth rate is observed with decreasing specimen thickness in the slow/rough region. Decreasing the specimen thickness will reduce dilatational stresses ahead of the crack tip hence reducing the extent of cavity growth. This would result in crack tips being sharper in thinner specimens, hence reducing the strain energy release rate necessary to drive a crack at a given rate as observed (Fig. 18a). At high crack growth rates if little cavity growth occurred, the crack tip diameter would be largely independent of specimen thickness, resulting in no specimen thickness effect as observed (Fig. 18a). It should be noted, however, that at low strain energy release rates for the thinnest specimen, slip/stick behaviour is still observed in this sulphur cured SBR, suggesting that cavitation is still significant.

The most highly swollen SBR-C material exhibited no slip/stick transition but had generally rough surfaces (Figs 9 and 10), suggesting that cavitation was occurring. Limited experiments were hence carried out to investigate the effect of specimen thickness on this behaviour as illustrated in Fig. 19. The thin material showed clear slip/stick behaviour suggesting that the thickness effect was to reduce dilatational stresses hence tending to reduce the extent of cavitation.

Crack growth rate experiments were carried out on the SBR-C material filled with 50 phr carbon black (SBR-F), for two specimen thicknesses. The results are shown in Fig. 20. It is clear from these data that no specimen thickness effect is observed. This is not

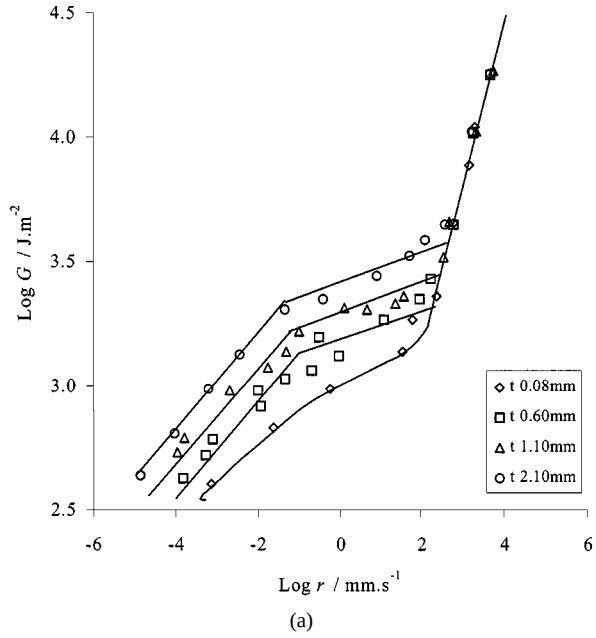

(a)

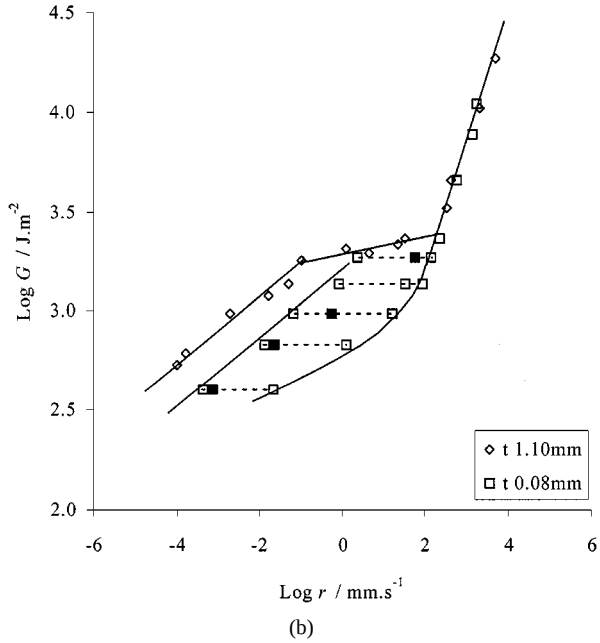

(b)

Figure 18 (a) The effect of specimen thickness on the strain energy release rate (G) versus tear rate (r) relationship for SBR-C showing only the average values of r plotted in the stick-slip region. (b) Some of the data from Fig. 18a re-plotted to illustrate the slow/fast crack growth behaviour in the stick-slip region (B) for the thinnest specimen.

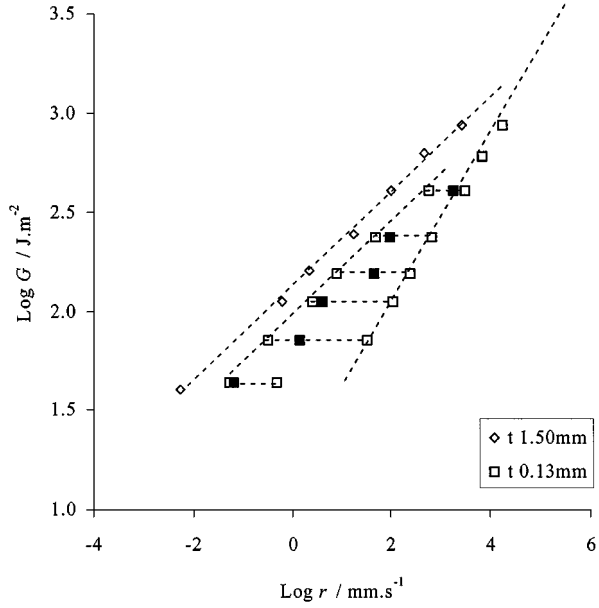

Figure 19 The effect of specimen thickness on the strain energy release rate (G) versus tear rate (r) relationship for SBR-C swollen with Dibutyl Adipate to $V_r = 0.38$.

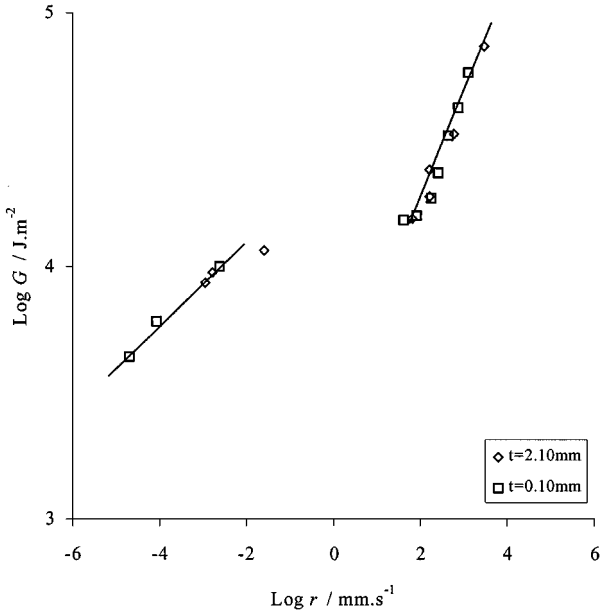

Figure 20 The effect of specimen thickness on the strain energy release rate (G) versus tear rate (r) relationship for SBR filled with 50 phr. HAF carbon black (compound F).

surprising at the high crack growth rates in the smooth region, as cavitiation effects will not be present. At low crack growth rates in this material relatively smooth surfaces were observed (Fig. 10), although the possibility of a roughness being present on a scale below that observable in the present optical micrographs cannot be ruled out. For both specimen thicknesses a discontinuity is observed in the measured crack growth rates (Fig. 20) which suggests a change in crack growth mechanism. It may be that cavitation does occur in this highly hysteretic material at the relatively high strain energy release rates but that the cavities that grow are numerous but small compared to the specimen thickness.

4. Conclusions

The relationship between the strain energy release rate (G) necessary to drive a crack and the consequent crack growth rate or tear rate (r) is found to be of the form illustrated in Fig. 2 for most of the materials studied.

In region C where rapid steady tearing occurs producing smooth surfaces, it is likely that the increase in the magnitude of G necessary to drive a crack at higher rates arises from an increase in magnitude of the viscoelastic work that has to be done in the crack tip region rather than from an increase in crack tip diameter. This is evidenced by the fact that the data in this region scale with the WLF relationship for both unfilled (Fig. 13b) and filled materials (Fig. 14b). The value of G decreases

with the extent of swelling in a manner proportional to the decrease in the loss modulus (Fig. 5). Finally the contention is further supported by the fact that the value of G necessary to drive a crack at a given rate increases with the average molar mass between crosslinks in the same manner for both peroxide and sulphur cured materials (Fig. 17). In region A rough surfaces are observed and it has been postulated that the origin of the roughness may be cavitation ahead of the crack tip due to dilatational stresses (21, 30–32). In this region the extending crack would intersect with growing cavities causing an increase in crack tip diameter and hence an increase in the magnitude of G. This hypothesis is supported by the specimen thickness effects reported here. In the unswollen materials (Fig. 18) in region A, the value of G necessary to drive a crack at a given rate decreases with decreasing specimen thickness in a manner that would be expected from the decrease in magnitude of the dilatational stresses and hence propensity to cavitate. In region C, however, the value of G is independent of specimen thickness suggesting that cavitation either does not occur or has little effect on crack tip geometry. Even in highly swollen materials (Fig. 19) reducing the thickness results in a decrease in the magnitude of G and a change from rough to slip/stick behaviour. In carbon black materials the fracture surfaces do not appear very rough even at low tear rates and there appears to be no effect of specimen thickness (Fig. 20). However, there is a clear transition in the G versus r behaviour with a significant discontinuity (Figs 9 and 20). Furthermore it is not possible to superpose the temperature rate data with the WLF relationship suggesting that in the low tear rate region (Fig. 14b) there is a significant crack tip effect. It may be that the cavities which may have formed were too small to affect the surface roughness on the optical microscope scale. The extent and nature of the slip/stick transition region is clearly affected by the materials variables. It becomes a discontinuity for carbon black filled materials (Fig. 9) but tends to reduce in extent with both extent of swelling (Fig. 9) and with increasing crosslink density (Figs 15 and 16). It appears that as visco-elastic losses decrease the crack tip profile effect on crack growth rate reduces significantly.

Acknowledgements

One of the authors, K. Tsunoda would like to thank the Bridgestone Corporation, Japan for giving him leave of absence, financial support and materials/experimental support while he carried out this work during his PhD studies at Queen Mary and Westfield College, University of London.

Dedication

One of the authors, Alan G. Thomas knew Andrew from the time that he arrived in the U.K. and another, Craig K.L. Davies from about 1970. Our associations were broad ranging, personal and professional, including collaborative work, conferences, PhD examinations, EPSRC Committees, refereeing etc. Andrew was a gentleman, always pleasant, often amusing and always clear thinking. He was an excellent storyteller particularly when recounting stories of his own experiences around the world. Andrew was very much a family man—his family was vital to him. He has made an enormous contribution to polymer science, particularly in the area of polymer crystal structure/crystallisation and associated processing/structure/property relationships. He was creative, very productive, often with real sparks of insight. Andrew was forceful and persuasive of his ideas but always in a quiet, convincing, enthusiastic manner. He could and would talk to anyone from student to Nobel Laureate always being willing to give of his time. Andrew was a genuine scientist, a little unworldly who lived in and for his subject. He was a one off who will be sorely missed, but his contribution to the subject will continue to make a major impact for many years to come and will remain forever.

References

1. A. G. THOMAS, Goodyear Medal Paper presented to the American Chemical Society Rubber Division Meeting Chicago, April 1994; *Rubber Chem. Technol.* **67** (1994) G50.
2. G. J. LAKE, *Rubber Chem. Technol.* **68** (1995) 432.
3. R. S. RIVLIN and A. G. THOMAS, *J. Polym. Sci.* **10** (1953) 291.
4. A. G. THOMAS, *J. Appl. Polym. Sci.* **3** (1960) 168.
5. L. MULLINS, *Trans. Inst. Rubber. Ind.* **35** (1959) 213.
6. E. H. ANDREWS and Y. FUKAHORI, *J. Mater. Sci.* **12**. (1977) 1307.
7. A. N. GENT and S. M. LAI, *J. Polym. Sci. Polm. Phys. Ed* **32** (1994) 1543.
8. A. G. THOMAS, *J. Polym. Sci.* **18** (1955) 177.
9. A. N. GENT and A. W. HENRY, in Proc. 5th Int. Rubber Conf., Brighton (Pub. Maclaren, London, 1967) p. 193.
10. M. L. WILLIAMS, R. F. LANDEL and J. D. FERRY, *J. Am. Chem. Soc.* **77** (1955) 3701.
11. G. J. LAKE and A. G. THOMAS, *Proc. R. Soc. London Ser* **A300** (1967) 108.
12. G. J. LAKE and P. B. LINDLEY, *Rubber J.* **152**(10) 24; **152**(11) (1964) 30.
13. A. AHAGON and A. N. GENT, *J. Polym. Sci. Polym. Phys. Ed.* **13** (1975) 930.
14. A. N. GENT and R. H. TOBIAS, *ibid.* **20** (1982) 2051.
15. A. K. BHOWMICK, A. N. GENT and C. T. R. PULFORD, *Rubber Chem. Technol.* **56** (1983) 226.
16. G. J. LAKE and P. B. LINDLEY, *J. Appl. Polym. Sc.* **10** (1966) 343.
17. K. A. MAZICH, M. A. SAMAS, C. A. SMITH and G. ROSSI, *Macromolecules* **24** (1991) 2766.
18. G. J. LAKE and O. H. YEOH, *J. Polym. Sci. Part B. Polymer Physics* **25** (1987) 1157.
19. A. N. GENT, S. M. LAI, C. NAH and CHI WANG, *Rubber Chem. Technol.* **67** (1994) 610.
20. A. N. GENT and H. J. KIM, *ibid.* **51** (1978) 35.
21. J. J. C. BUSFIELD, C. H. RATSIMBA and A. G. THOMAS, *J. Nat. Rubb. Res.* **12**(3) (1997) 131.
22. A. KADIR and A. G. THOMAS, *Rubber Chem. Technol.* **54** (1981) 15.
23. A. N. GENT and P. B. LINDLEY, *Proc. R. Soc. London Ser A* **249** (1958) 195.
24. A. N. GENT and D. A. TOMPKINS, *J. Appl. Phys.* **40** (1970) 2520.
25. J. M. BALL, *Phil. Trans. R. Soc. Ser A* **306** (1982) 557.
26. A. N. GENT and C. WANG, *J. Mat. Sci.* **26** (1991) 3392.
27. H. S. HOU and R. ABEYARATNE, *J. Mech. Phys. Solids* **40** (1992) 571.
28. J. F. GANGHOFFER and J. SCHULTZ, *Rubber Chem. Technol.* **68** (1995) 757.

29. J. J. C. BUSFIELD, C. K. L. DAVIES and A. G. THOMAS, *Prog. Rubber and Plastics Technol.* **12**(3) (1996) 191.
30. G. J. LAKE, C. C. LAWRENCE and A. G. THOMAS, *Polymer* **33** (1992) 4069.
31. *Idem.*, in Proc. Int. Rubber Conf., Brighton (Plastics and Rubber Institute, 1992) p.71.
32. *Idem.*, *Rubber Chem. Technol.*, submitted.
33. K. AKUTAGAWA, C. K. L. DAVIES and A. G. THOMAS, *Prog. Rubber and Plastics Technol.* **12** (1996) 174.
34. J. J. C. BUSFIELD, C. DEEPRASERTKUL and A. G. THOMAS, *Polymer*, accepted for publication.
35. D. K. DE, Ph.D thesis, Queen Mary and Westfield College, University of London, UK, 1994.
36. K. AKUTAGAAWA, Ph.D thesis, Queen Mary and Westfield College, University of London, UK, 1995.
37. G. R. HAMED, *Rubber Chem. Technol.* **67** (1994) 529.
38. A. N. GENT and C. T. R. PULFORD, *J. Mater. Sci.* **19** (1984) 3612.
39. G. J. LAKE and O. H. YEOH, *Int. J. Fract.* **14** (1978) 509.

Received 29 February
and accepted 2 March 2000